

Single- and double-electron capture from many-electron atoms by α particles in the MeV energy range

V. V. Afrosimov, D. F. Barash, A. A. Basalaev, N. A. Gushchina, K. O. Lozhkin,
V. K. Nikulin, M. N. Panov, and I. Yu. Stepanov

A. F. Ioffe Physico-technical Institute, Russian Academy of Sciences, 194021 St. Petersburg, Russia
(Submitted 12 April 1993)

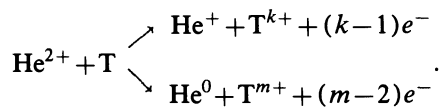
Zh. Eksp. Teor. Fiz. **104**, 3297–3310 (October 1993)

Analysis of the charge composition of an ion beam is used to measure the cross sections of single- and double-electron capture processes when ${}^3\text{He}^{2+}$ ions interact with atoms of He, Ne, Ar, Kr, and Xe and molecules of N_2 in the collision energy range 0.1–2.5 MeV/amu. For such systems the cross sections of single- and double-electron capture are calculated by the target continuum distorted-wave method in the independent particle model. Interelectron interactions are taken into account by choosing the wave functions in the Hartree-Fock approximation with matched effective charges. The partial cross sections for capture into excited states are calculated. The experimental and theoretical results obtained are found to be in satisfactory agreement.

1. INTRODUCTION

Electron capture processes in collisions of fast ($v > 1$ au) ions with atoms and molecules play an important role in the transport of ion beams, and can also be used to obtain high-energy atomic beams. Of especial interest are data on the interaction of fast α particles with He atoms, in connection with the important role of the helium component of high-temperature plasmas in thermonuclear devices.

When α particles collide with atoms of a target T , two groups of elementary processes, accompanied by the formation of fast He^+ and He^0 atoms are possible:



Here $k=1$ in the first reaction corresponds to single-electron capture and $m=2$ in the second reaction corresponds to double-electron capture. For $k > 1$ and $m > 2$ the capture processes are accompanied by ionization of the target atoms.

To measure the cross sections of all the elementary processes involving change of the charge state of the collision partners, it is necessary to use coincidence methods. However, for most practical applications it is necessary to have information about the charge states of only the fast particles formed in the collision process. In turn, theoretical studies of electron capture processes usually do not consider the final charge state of the slow many-electron particle. For this reason, in the present paper we use the simple method involving analysis of the charge composition of an ion beam which has passed through a gaseous target under conditions such that only one collision occurs to measure the total single- and double-electron capture cross sections.

In the calculation of the cross sections of capture of one and two electrons by fast α particles from many-electron atoms it is necessary to take into account the

many-electron structure of the target, and also the possibility of capture into excited states of the fast particle (the projectile). In the computation of a large number of partial cross sections it is desirable to have a computational method which is universal and does not require a significant amount of machine time. In the region of high-energy particle collisions the target continuum distorted-wave (TCDW) approximation, developed in Refs. 1–4, which allows an analytic representation of the transition amplitude $T(n_i l_i m_i \rightarrow n_f l_f m_f)$ between arbitrary hydrogen-like states in the form of a finite sum,⁴ proves to be effective.

In the TCDW approximation the wave functions and perturbing potentials in the initial and final channels of the charge-transfer reaction are chosen in equivalently. The wave function of the initial state is chosen in the form of a moving atomic orbital, and the wave function of the final state coincides with the continuum distorted-wave (CDW) function and takes account of the influence of the long-range Coulomb potential of the target. The Coulomb interaction of an active target electron with the incident particle constitutes a perturbation in the initial channel. Crothers *et al.*⁵ have shown that the TCDW approximation is the high-energy limit of the variational distorted-wave approximation with a center point (half-way house variational CDW), which has regular boundary conditions and does not contain any divergences in the second- or higher-order perturbation theories.

Application of the first order TCDW approximation in the hydrogen orbital basis to the description of the capture by protons of $1s$ electrons from hydrogen and a series of many-electron atoms gives good agreement with experimental data not only for the total,³ but also the angular differential cross sections.⁵

The above considerations testify in favor of our choice of the TCDW approximation to calculate the cross sections of electron capture from many-electron targets, even though we have allowed for the long-range Coulomb distortion only in the final channel of the charge-transfer reaction. An adequate description of the many-electron

structure of the atomic target is achieved by use of the Hartree–Fock (HF) basis functions.⁶

2. EXPERIMENTAL TECHNIQUE

To measure the cross sections of single- and double-electron capture processes, we used the method of ion beam charge composition analysis. In this method the ion beam is passed through a gaseous target. ${}^3\text{He}^{2+}$ ions, used in the experiment to reconstitute H_2^+ ions from the mixture, were obtained in an arc source and accelerated in the 120-centimeter cyclotron at the Ioffe Physico-technical Institute, which has a maximum energy of 6.75 MeV/amu. After acceleration, the ions are passed through a magnetic mass-monochromator, which cleanses the beam of singly charged impurity ions and atoms formed during passage through the accelerator. Next, the ion beam is directed into the collision chamber, which is filled with the gaseous target. The density of the target in the collision chamber is set to ensure single collisions. The absolute pressure was measured to within 15%.

The particles, after passing through the collision chamber, were charge-analyzed with a magnetic analyzer. For simultaneous recording of the reaction products (He^+ ions and He atoms), two detection channels were used, operating in the counting regime. The recording efficiency was $86 \pm 5\%$. Simultaneously, the intensity of the primary beam was measured in the current regime to within 5%. The measurement error of the magnitude of the cross sections is estimated to lie in the range 17–20%.

3. COMPUTATIONAL TECHNIQUE

In the TCDW approximation the amplitude of the single-electron capture process in the wave description has the form³

$$\begin{aligned} T(q) &= N(v_T^f) \int d\mathbf{r}_T \exp(i\mathbf{Q}\mathbf{r}_T) \Phi_i(\mathbf{r}_T) {}_iF_1 \\ &\quad \times (iv_T^f; 1; iv_T + iv_T) \int d\mathbf{r}_P \Phi_f^*(\mathbf{r}_P) V_i(\mathbf{r}_P) \\ &\quad \times \exp(-i\tilde{\mathbf{Q}}\mathbf{r}_P) \\ &= N(v_T^f) I\tilde{I}, \end{aligned} \quad (1)$$

where the normalization factor $N(v_T^f)$ of the distorted wave function of the final state is given by

$$N(v_T^f) = \exp(\pi v_T^f/2) \Gamma(1 - iv_T^f), \quad (2)$$

where $v_T^f = Z_P^f/v$, $\mathbf{v} = v\hat{\mathbf{v}}$ is the collision velocity, and Z_P^f is the charge of the long-range Coulomb potential of the target in the final channel. For the vectors \mathbf{Q} and $\tilde{\mathbf{Q}}$ we have⁷

$$\begin{aligned} \mathbf{Q} &= q\hat{\mathbf{i}} + \tilde{\beta}\hat{\mathbf{v}}, \quad \tilde{\beta} = \Delta\varepsilon/v - v/2; \\ \tilde{\mathbf{Q}} &= q\hat{\mathbf{i}} + \beta\hat{\mathbf{v}}, \quad \beta = \Delta\varepsilon/v + v/2. \end{aligned} \quad (3)$$

The quantity $\Delta\varepsilon = \varepsilon_f - \varepsilon_i$ is the difference between the energies of the final and initial bound states, q is the transverse component of the momentum transfer (the vector $\hat{\mathbf{i}}$ is perpendicular to the vector $\hat{\mathbf{v}}$ and lies in the collision

plane). The perturbation $V_i(\mathbf{r}_P) = -Z_P^i/r_P$ in the initial channel corresponds to the Coulomb interaction of the electron with the incident ion. The function $\Phi_i(\mathbf{r}_T)$ describes the bound state of the electron on the target and is chosen in the Hartree–Fock approximation,⁶ the function $\Phi_f(\mathbf{r}_P)$ describes the bound state of the electron on the projectile and is represented by a hydrogen-like orbital; \mathbf{r}_T and \mathbf{r}_P are the radius vectors of the electron relative to the target or projectile nucleus, respectively, and I and \tilde{I} are three-dimensional integrals, analytic expressions for which are given in the Appendix.

In the numerical calculations of the single-electron capture cross sections we used the following values of the model parameters: $Z_P^i = 2$, $Z_P^f = 2$; the HF-energy of the initial state ε_i was chosen from the tables in Ref. 6, and ε_f is the energy of the final state of the hydrogen-like ion with charge Z_P^f . The effective charge of the long-range distorting Coulomb potential of the target in the final channel was taken, following Ref. 1, to be $Z_T^f = n_i \sqrt{2|\varepsilon_i|}$.

The total cross section of single-electron capture was calculated by summing over the partial cross sections of all the excited states of the fast He^+ ion and all the shells of the target particle. The channels connected with the formation of the excited states of the projectile were taken into account only in those cases in which their contribution to the total cross section did not go below 1%.

In the calculation of the cross section of double-electron capture, we used the independent-particle model, in which the probability of capture is calculated as the product of the probabilities of single-electron capture for each of the active electrons of the target $e^-(1)$ and $e^-(2)$.

In the calculations of the double-electron capture cross sections we used the parameters $Z_P^i(1) = Z_P^i(2) = 2$; $\varepsilon_i(1)$ and $\varepsilon_i(2)$ were chosen for the corresponding states of the neutral atoms, i.e., the effects of realignment of the atomic shell of the target during the collision were not taken into account; the use of $Z_P^i(1) = Z_P^i(2) = 1.69$ for capture to $1s^2$ state and $Z_P^f(1) = 2$, $Z_P^f(2) = 1$ for capture to the $(1s, n_f l_f m_f)$ state with $n_f \geq 2$ for the second electron is connected with the treatment of the interelectron interaction in the final channel; the Coulomb charges $Z_T^i(1)$, $Z_T^f(2)$ of the long-range distortion were determined as in the case of single-electron capture from the energies $\varepsilon_i(1)$, $\varepsilon_i(2)$ of the initial HF-states of the electrons $e^-(1)$ and $e^-(2)$, respectively; the energies of the final hydrogen-like states $\varepsilon_f(1)$ and $\varepsilon_f(2)$ were determined by using the corresponding charges $Z_P^f(1)$ and $Z_P^f(2)$.

The total double-electron capture cross section was calculated as the sum of the partial cross sections of the singly excited states of the final channel and all possible pairs of target electrons. For a helium target we included the singly excited channels up to $n_f = 4$, and for other targets we cut the sum off at $n_f = 2$.

4. RESULTS AND DISCUSSION

4.1. Single-electron capture

Experimental values of the total cross sections for single-electron capture and the calculated total and partial

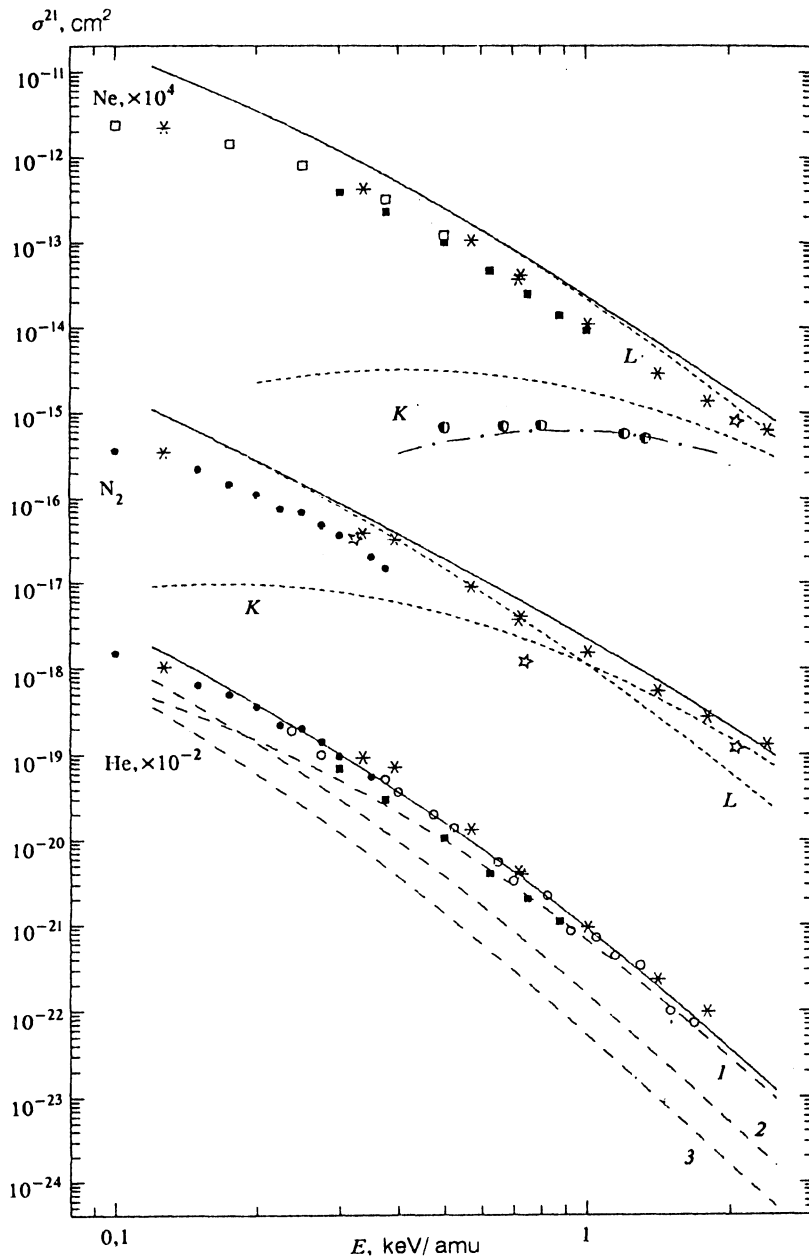


FIG. 1. Cross sections of single-electron capture in the collisions ${}^3\text{He}^{2+} + \text{He}$, N_2 , Ne . Experiment: *—results of the present work, ●—Ref. 8, ○—Ref. 9, ☆—Ref. 10, □—Ref. 11, ■—Ref. 12, ⊙—Ref. 14. Theoretical results of the present work: solid curves—total cross sections, long-dashed curves—partial cross sections of capture to the states $n_f=1, 2, 3$ of the fast ion, short-dashed curves—partial cross sections of capture from various shells of the target; dot-dashed curve—cross section of capture from the K shell of neon to the ground state of the fast ion.¹³

electron-capture cross sections for collisions of He^{2+} ions with atoms of He, Ne, Ar, Kr, Xe, and molecules of N_2 are shown in Figs. 1 and 2. Satisfactory agreement is observed between our results and the available experimental data⁸⁻¹² obtained for individual sections of the collision energy range considered here.

In the velocity region ($2 < v < 22$ a.u.) under consideration the cross sections σ^{21} decrease rapidly as functions of the collision velocity for all targets, but, as can be seen from these data, there are flat stretches in the curves of the total cross sections plotted as functions of collision energy. This effect is particularly striking for Ar, Kr, and Xe (Fig. 2). Calculations of the partial electron-capture cross sections show that these peculiarities in the total cross sections arise at collision energies such that the contributions of the processes of electron capture from the various shells

of the target become comparable in magnitude (Figs. 1 and 2).

The magnitude of the cross section for electron capture from a many-electron atom is determined not by the total number of electrons in the atom, but by the number of electrons in the shell from which there is the greatest probability of capture. For example, as can be seen from our calculations, in the region of high collision energies ($E \sim 1$ MeV/amu), when α particles interact with Ar atoms capture takes place preferentially from the L shell which has 8 electrons, and the capture cross section is roughly half that for Kr atoms, for which the process is determined by the 18 electrons of the M shell. On the other hand, in the same range of collision velocities the cross sections of electron capture from Kr and Xe atoms are close in magnitude, which is explained by the defining role of the N shell of

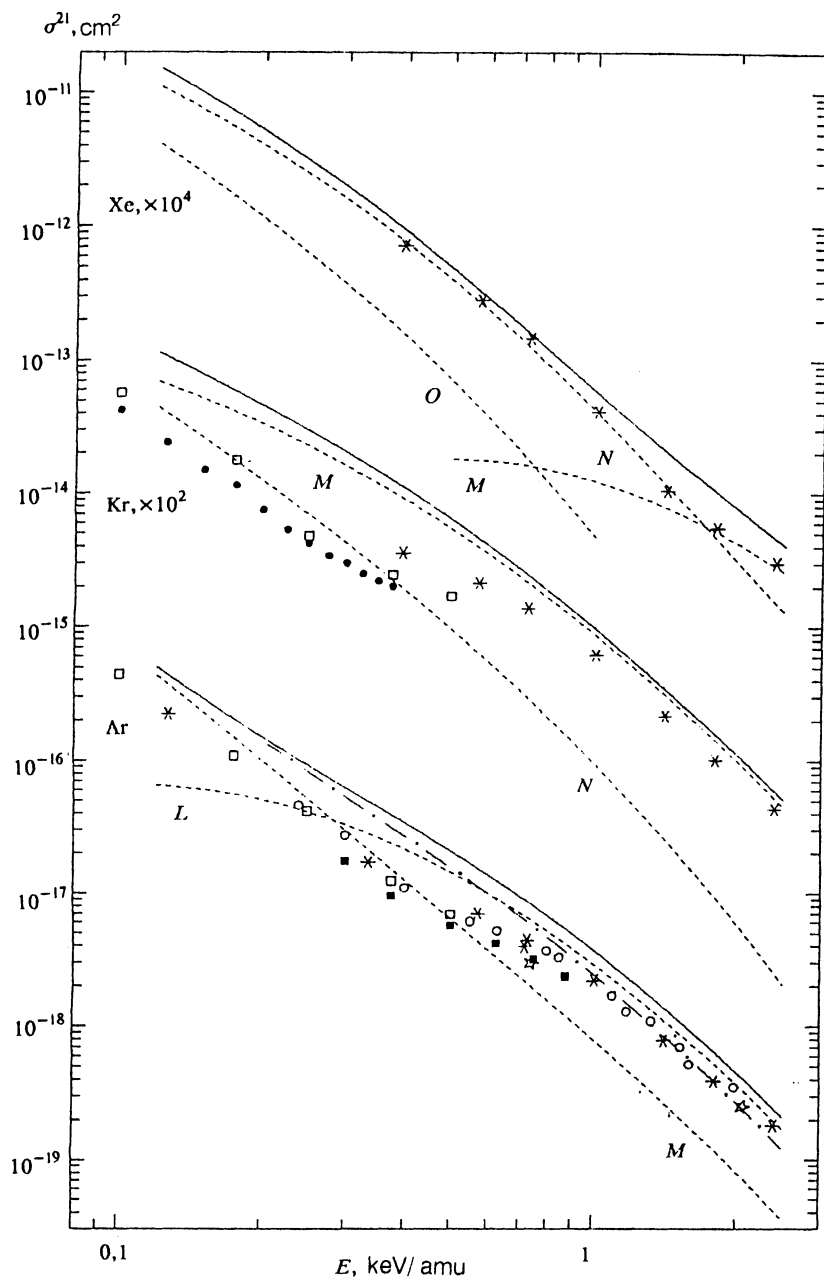


FIG. 2. Cross sections of single-electron capture in the collisions ${}^3\text{He}^{2+} + \text{Ar}, \text{Kr}, \text{Xe}$. Dot-dashed curve—total cross section of capture from an argon atom, calculated in Ref. 1, all else as in Fig. 1.

xenon, which also has 18 electrons (Fig. 2).

Comparing the experimental and theoretical results obtained in this work, we are able to draw some conclusions about the region of applicability of the TCDW high-energy approximation. For example, the experimentally obtained cross section for electron capture from an atom of Ar shows a flat stretch in the collision energy region $E \sim 0.5$ MeV/amu, which corresponds roughly to the velocity range of the electrons in the L shell of Ar. It is specifically at these collision energies that the greatest difference between the theoretical and experimental results is found for the given pair. In the region of lower collision energies, where, in the given example, electron capture from the M shell of argon plays a decisive role, agreement with experiment improves significantly. In our opinion, the reason for this is that the TCDW approximation overestimates the partial cross sections at collision velocities near

the orbital velocities of the electrons of the corresponding shells, and predicts that the maxima of the partial cross sections should be found at lower collision velocities than are needed to explain the experimental data. Use of the more cumbersome (from the computational point of view) CDW approximation¹ yields qualitatively analogous results both for the total (Fig. 2) and for the partial capture cross sections. Agreement of the theoretical results of Ref. 1 with the experimental data in the high-energy region is somewhat better, which is explained by noting that the long-range Coulomb distortion is taken into account in the initial channel.

These shortcomings of the theory can be attributed to violation of the condition of normalization of the distorted wave function in the low-velocity region (in comparison with the orbital velocity of the captured electron), and also by the rather rough way in which the long-range distorting

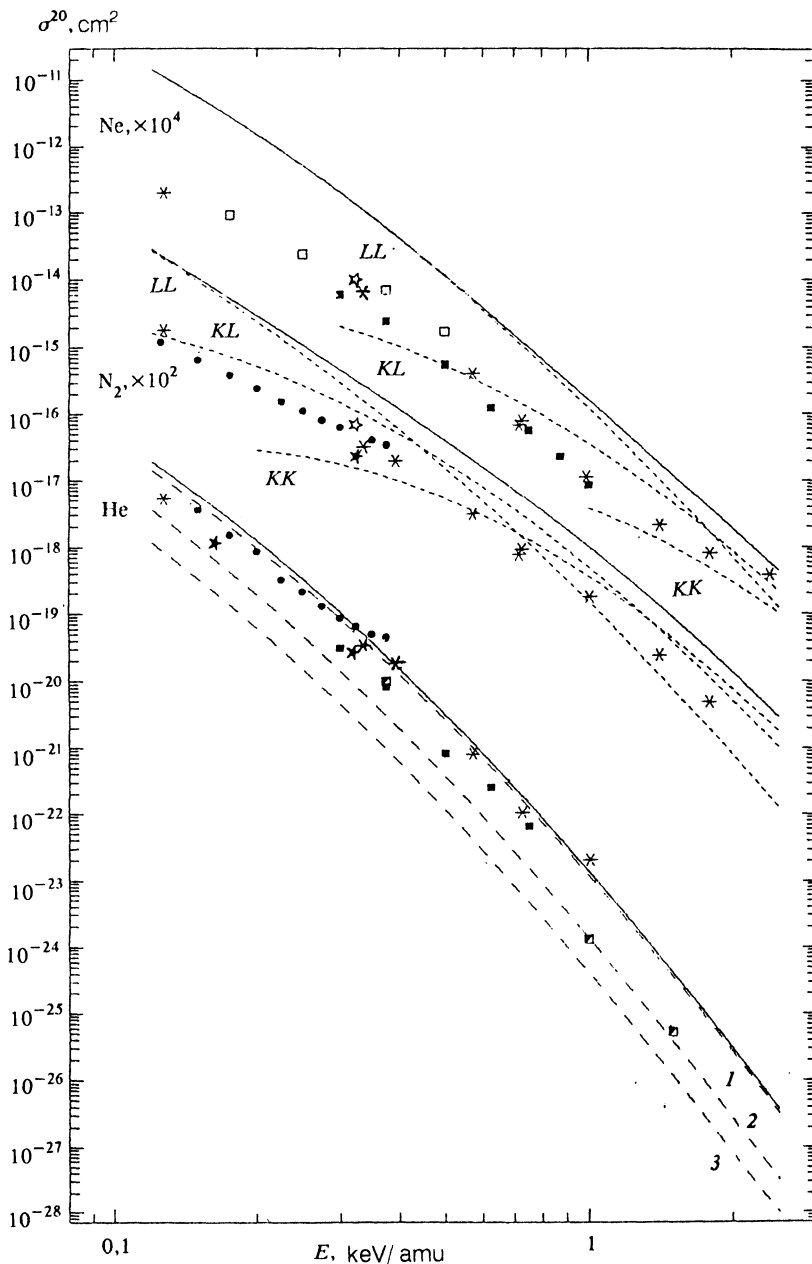


FIG. 3. Cross sections of double-electron capture in the collisions ${}^3\text{He}^{2+} + \text{He}, \text{N}_2, \text{Ne}$. Experiment: *—results of the present work, ●—Ref. 8, ☆—Ref. 10, □—Ref. 11, ■—Ref. 12, *—Ref. 18, ◻—Ref. 19. Theoretical results of the present work: solid curves—total cross sections, long-dashed curves—partial cross sections of capture to the states $(1s, n_r(2)=1,2,3)$ of the fast ion, short-dashed curves—partial cross sections of capture from various shells of the target.

potential of the target is approximated in the final channel.

An important step forward, which allows us to correctly describe the behavior of the partial cross sections in the region of the maximum by perturbation theory methods, is the procedure of wave-packet renormalization, which takes into account the three-body nature of the interaction (extrashell effects). This approach was proposed by Marxer and Briggs¹³ and used by them within the framework of the strong-potential Born approximation (the renormalized strong-potential Born approximation—RSPB) to calculate the cross sections of electron capture from the *K* shell of neon to the ground state of He^+ . The results obtained using the RSPB approximation give a significantly smaller cross section in the region of the maximum in comparison with the SPB approximation without renormalization¹³ and the TCDW approximation, and are

in good agreement with the experimental data of Rødbro *et al.*¹⁴ (Fig. 1).

The TCDW approximation, as can be seen from Fig. 1, does a good job of describing the electron capture process in the simple many-electron system $\text{He}^{2+} + \text{He}$. This is because the entire energy region under consideration falls entirely within the region of applicability of the method, as a consequence of the relatively low orbital velocity of the electrons.

Our theoretical results show that the contribution of processes leading to the formation of excited states of the fast ion to the total cross section dominates at small velocities, increasing with the velocity; however, even for $E=2.0$ MeV/amu it stands at around 20%. The similar behavior of the cross sections holds also for other targets, which

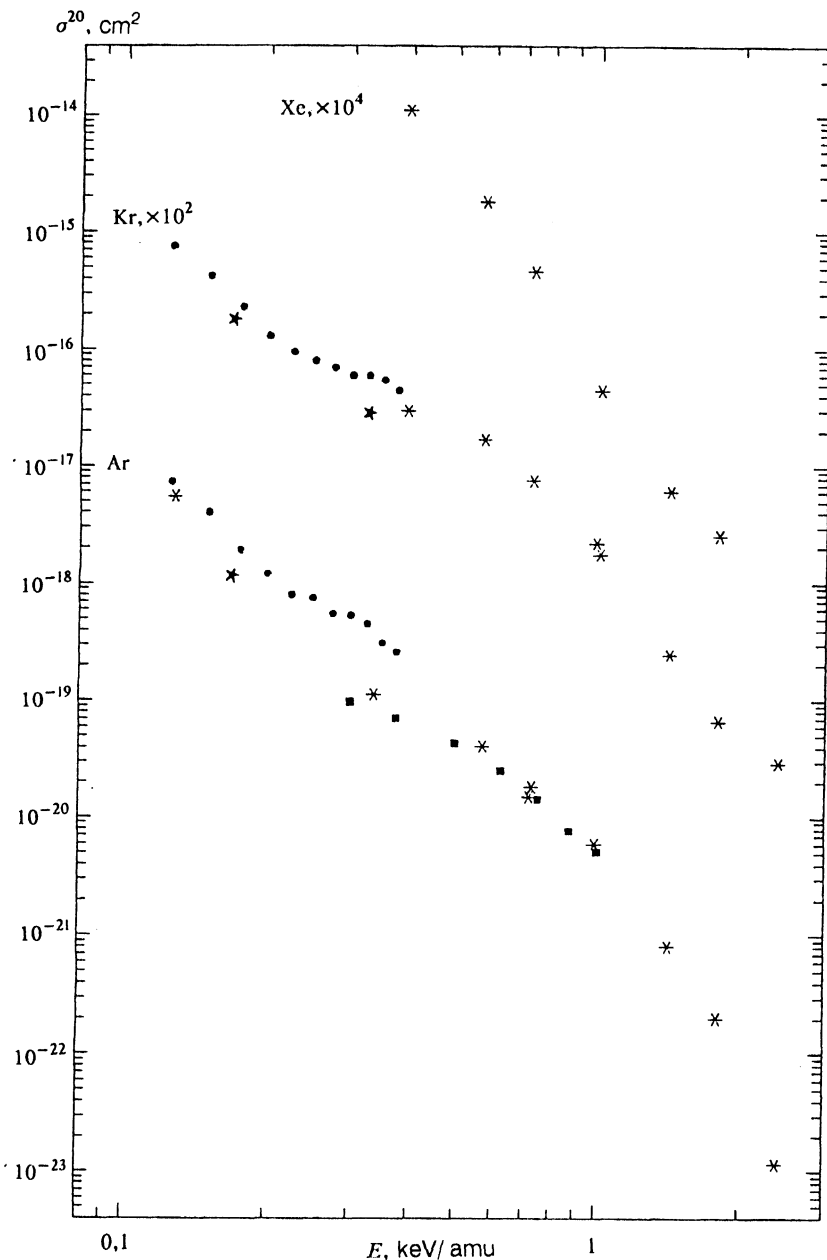


FIG. 4. Cross sections of double-electron capture in the collisions ${}^3\text{He}^{2+} + \text{Ar, Kr, Xe}$. Experiment: notation as in Fig. 3.

points up the importance of taking account of capture to excited states.

A large number of papers (see Refs. 1, 15–17) have been dedicated to calculations of the cross sections of single-electron capture in the $\text{He}^{2+} + \text{He}$ system at high energies. The results obtained in the first-order perturbation theory in different variants of the distorted-wave formalism are in satisfactory agreement with each other and with experiment. The total and partial cross sections which we have obtained are found to be in good agreement (to within 25–30%) with the theoretical results of Belkić¹⁷ who used the first Born approximation with correct boundary conditions (the correct first Born approximation—CB1) with Hartree–Fock orbitals for the initial state, and with increase of the collision energy this agreement improves.

4.2. Double-electron capture

The total cross sections σ^{20} for double-electron capture from He, Ne, Ar, Kr, and Xe atoms and N_2 molecules which we have obtained are shown in Figs. 3 and 4. Our experimental data are in satisfactory agreement with the results of Refs. 8, 10–12, 18, and 19.

In the investigated range of collision velocities the cross sections σ^{20} decrease rapidly with increase of the collision velocity. Features are also observed in the dependence of the double capture cross sections which are due to electron capture from different shells, albeit less pronounced than in the case of single-electron capture. On the basis of our calculations for Ne and N_2 this can be explained qualitatively by the presence of a noticeable contribution from the reaction channel corresponding to cap-

ture of electrons belonging to different shells of the target atom (the *KL* curves in Fig. 3).

For the many-electron targets N_2 and Ne it can be seen that our calculated total cross sections substantially exceed the experimental values (Fig. 3). As one goes to heavier targets, this difference grows. The reason for these discrepancies, in our view, may be a not entirely correct choice of the charge Z_T^f of the long-range Coulomb potential of the target distorting the electron wave function in the final channel of the charge-transfer reaction, and also violation of the normalization condition of the distorted wave function,¹³ which leads to a still greater overestimate of the cross sections than in the case of single-electron capture.

Despite the obvious limitations of the independent particle model, the total cross section which we have calculated for double-electron capture from an atom of He is in good agreement with the experimental data (Fig. 3). The calculation shows that over the entire range of collision velocities examined the process that determines the magnitude of the cross section is the one that leads to the formation of a fast helium atom in the ground state. The velocity dependence of the cross sections for capture to singly excited states of He ($1s, n=2-4$) is similar to that for capture to the ground state, but the magnitude of the cross sections falls off rapidly with growth of the principal quantum number of the excited electron.

Our theoretical results are in good agreement with the calculations of other authors.¹⁹⁻²² Calculations based on the CDW approximation taking account of static electronic correlations in the initial channel¹⁵ give cross sections which are 1.5-2 times smaller than calculations based on the independent particle model, and at large energies far smaller than the corresponding experimental data. Dunseath and Crothers¹⁵ tie this fact to the necessity of accounting for capture to excited states of the projectile. However, as follows from Fig. 3 and the data of Ref. 20, the contribution of excited states to the total cross section, in contrast to the case of single-electron capture, is small and amounts to only about 10%.

An effort to account for dynamic as well as static correlations in the description of double-electron capture in the system $He^{2+} + He$ was undertaken in Ref. 23, in which the formal theory of single-electron capture, formulated within the framework of the three-body problem, was generalized to the case of double-electron capture, as a correct theory of the four-body problem. The results obtained in this generalized CB1 approximation allow one to conclude that dynamic correlations do not significantly affect the magnitude of the total cross section.

5. CONCLUSIONS

The collision energy range chosen for study allows us, on the basis of the experimental data, to draw some conclusions about the role of capture from different shells of the target particles, but only concerning the total cross sections.

The agreement between our experimental and theoretical results highlights the effectiveness of using the target

continuum distorted-wave (TCDW) approximation with a basis of Hartree-Fock wave functions for the initial state in calculations of the partial cross sections of electron capture by fully stripped ions in the MeV energy range from neutral atoms in the region of collision velocities greater than the velocity of the electrons of the corresponding shells of the target atoms. Further refinement of the given approximation within the framework of the independent particle model depends on to renormalization of the distorted wave function of the final state and correct choice of the long-range distorting target potential.

The authors thank their coworkers at the cyclotron laboratory of the Ioffe Physico-technical Institute—G. M. Gusinskiĭ, D. B. Korsakov, L. A. Rassadin, and O. M. Fëdotov for help in carrying out the experiments, and also Yu. B. Maïdel' and E. A. Orlov for help in setting up the experiment. Three of us (A. A. B., K. O. L., and I. Yu. S.) express our gratitude for partial financial support of this work provided by the Soros fund under the aegis of the American Physical Society.

6. APPENDIX. ANALYTIC EXPRESSION FOR THE AMPLITUDE OF SINGLE-ELECTRON CAPTURE

Substituting in Eq. (1) the expression for the wave function of the initial state $\Phi_i(r_T)$ in the Hartree-Fock approximation⁶ ($n_l m = n_l l_j m_j$)

$$\begin{aligned} \Phi_i(r_T) &= \Phi_{nlm}(r_T) = \sum_s C_{nl}^s \chi_{nlm}^s \\ &= \sum_s \frac{C_{nl}^s}{(2n_l^s)!} (2\xi_l^s)^{n_l^s+1/2} r_T^{n_l^s} \\ &\quad \times \exp(-\xi_l^s r_T) Y_{lm}(\hat{r}_T), \end{aligned} \quad (A1)$$

and the expression for the wave function of the final state in the form of hydrogen-like orbitals ($n_l m = n_l l_j m_j$), after a number of lengthy transformations analogous to the transformations of Ref. 4, we obtain the following expression for the integral I for $n_l m = n_l l_j m_j$:

$$\begin{aligned} I &= 4 \sqrt{2\pi(2l+1)(l+m)!(l-m)!} \sum_s C_{nl}^s \sqrt{\xi_l^s / (2n_l^s)!} \\ &\quad \times (n_l^s - 1)! \sum_{j=0}^{[(n_l^s-1)/2]} 4^{n_l^s-j} \frac{(n_l^s-j)!}{j!} \frac{1}{G^M} \left(1 - \frac{H}{G}\right)^{1-M-iv_T^f} \\ &\quad \times \sum_{l''=0}^{1-|m|} \frac{Q'' P_{l''0}(1) P_{l''m}(\cos(\hat{Q}\mathbf{v}))}{l''! \sqrt{(2l''+1)(2l''+1)(l''+m)!(l''-m)!}} \\ &\quad \times \sum_{h=0}^N \frac{(-1)^{j+h} l^{l+h}}{h!(N-h)!} \xi_l^{s(n_l^s+N-h)} \\ &\quad \times \sum_{k=0}^{M-l''-h-1} \frac{(l''+h+1-M)_k (1-iv_T^f)_k (iv_T^f)_{l''+h}}{k!(l''+h+k)!} \\ &\quad \times v^{l''+h} (H/G)^k, \end{aligned} \quad (A2)$$

and the following expression for the integral \tilde{I} for $n l m = n_f l_f m_f$:

$$\begin{aligned} \tilde{I} = & -4\lambda_f (-4i\lambda_f)^l Z_p^l \sqrt{(2\pi\lambda_f/n)(n-l-1)!(n+l)!} \\ & \times \tilde{Q}^l P_{lm}(\cos(\widehat{\mathbf{Q}}\mathbf{v})) \sum_{k=0}^{n-l-1} \frac{1}{(n-l-1-k)!(2l+1+k)!} \\ & \times \sum_{j=0}^{[k/2]} \frac{(-1)^{k+j} (l+k-j)!(2\lambda_f)^{2(k-j)}}{(k-2j)! j! (\lambda_f^2 + \tilde{Q}^2)^{k+l+1-j}}, \end{aligned} \quad (\text{A3})$$

where we have made use of the notation

$$\begin{aligned} G = & (\xi_i^s)^2 + \tilde{\beta}^2 + q^2, \quad M = n_i^s + 1 - j, \quad l'' = l_i - l', \\ H = & 2v(i\xi_i^s - \tilde{\beta}), \quad N = n_i^s - l_i - 2j, \quad \lambda_f = Z_p^f/n_f \end{aligned} \quad (\text{A4})$$

brackets denote integer part, P_{lm} are the normalized associated Legendre polynomials, and $(z)_k$ is the Pochhammer symbol, whose value is given by

$$(z)_0 = 1, \quad (z)_k = z(z+1)\dots(z+k-1). \quad (\text{A5})$$

Formula (A3) coincides with formula (13) of Ref. 4 after the elimination of typographical errors (an extraneous factor of $l_f!$).

¹Dž. Belkić, R. Gayet, and A. Salin, Phys. Rep. **56**, 279 (1979).

²D. S. F. Crothers and J. F. McCann, J. Phys. B **17**, L177 (1984).

³D. S. F. Crothers and K. M. Dunseath, J. Phys. B **20**, 4115 (1987).

⁴N. C. Deb, Phys. Rev. A **38**, 1202 (1988).

⁵D. S. F. Crothers and K. M. Dunseath, J. Phys. B **23**, L365 (1990).

⁶E. Clementi and C. Roetti, At. Data Nucl. Data Tabl. **14**, 177 (1974).

⁷D. S. F. Crothers and R. McCarroll, J. Phys. B **20**, 2835 (1987).

⁸L. I. Pivovarov, M. T. Novikov, and V. M. Tubaev, Zh. Eksp. Teor. Fiz. **42**, 1490 (1962) [Sov. Phys. JETP **15**, 1035 (1962)].

⁹P. Hvelplund, J. Heinemeier, E. H. Pedersen, and F. R. Simpson, J. Phys. B **9**, 491 (1976).

¹⁰I. S. Dmitriev, N. F. Vorob'ev, Zh. M. Konovalova *et al.*, Zh. Eksp. Teor. Fiz. **84**, 1987 (1983) [Sov. Phys. JETP **57**, 1157 (1983)].

¹¹R. D. Du Bois, Phys. Rev. A **36**, 2585 (1987).

¹²N. V. de Castro Faria, F. L. Freire, and A. G. de Pinho, Phys. Rev. A **37**, 280 (1988).

¹³H. Marxer and J. S. Briggs, J. Phys. B **25**, 3823 (1992).

¹⁴M. Rødbro, E. Horsdal-Pedersen, C. L. Cocke, and J. R. Macdonald, Phys. Rev. A **19**, 1938 (1979).

¹⁵K. M. Dunseath and D. S. F. Crothers, J. Phys. B **24**, 5003 (1991).

¹⁶A. A. Basalaeu, K. O. Lozhkin, V. K. Nikulin *et al.*, *Abstracts of Contributed Papers of the XVIIth Int'l. Conf. on the Physics of Electron-Atom Collisions* (Brisbane, 1991), ed. by I. E. McCarthy, W. R. MacGillivray, and M. C. Standage. Griffith University, Brisbane (1991), p. 610.

¹⁷Dž. Belkić, Physica Scripta **40**, 610 (1989).

¹⁸V. S. Nikolaev, L. N. Fateeva, I. S. Dmitriev, Ya. A. Teplova, Zh. Eksp. Teor. Fiz. **41**, 89 (1961) [Sov. Phys. JETP **14**, 67 (1961)].

¹⁹R. Shuch, E. Justiniano, H. Vogt *et al.*, J. Phys. B **24**, L133 (1991).

²⁰M. S. Gravielle and J. F. Miraglia, Phys. Rev. A **45**, 2965 (1992).

²¹R. Gayet, J. Hanssen, A. Martinez, and R. Rivarola, Z. Phys. D **18**, 345 (1991).

²²V. Yu. Lazur and Yu. Yu. Mashika, Zh. Tekh. Fiz. **61**, 25 (1961) [*sic*].

²³Dž. Belkić, Phys. Rev. A **47**, 189 (1993).

Translated by Paul F. Schippnick